Kinetic simulations of photogenerated charge transport in Cu based field emitter arrays for electron injector applications

Y. Iqbal[1] D. Guo[2] Y. Pokhrel[2] R. P. Joshi
[1]Department of Physics and Astronomy, Texas Tech University.
[2]Department of Electrical and Computer Engineering, Texas Tech University.

October 6, 2023

Introduction

Our research focuses on understanding charge transport in copper, with a particular emphasis on electron-electron and electron-phonon scattering effects. We use Monte Carlo simulations to calculate current density, incorporating transmission coefficients from Numerov solutions at the metal-vacuum interface. Additionally, we explore the integration of materials like carbon nanotubes into field emitter arrays to boost current output, while carefully addressing shielding effects caused by neighboring emitters. Our ultimate goal is to achieve higher current levels for electron injector applications. The basic scheme considered in this study is given in [1].

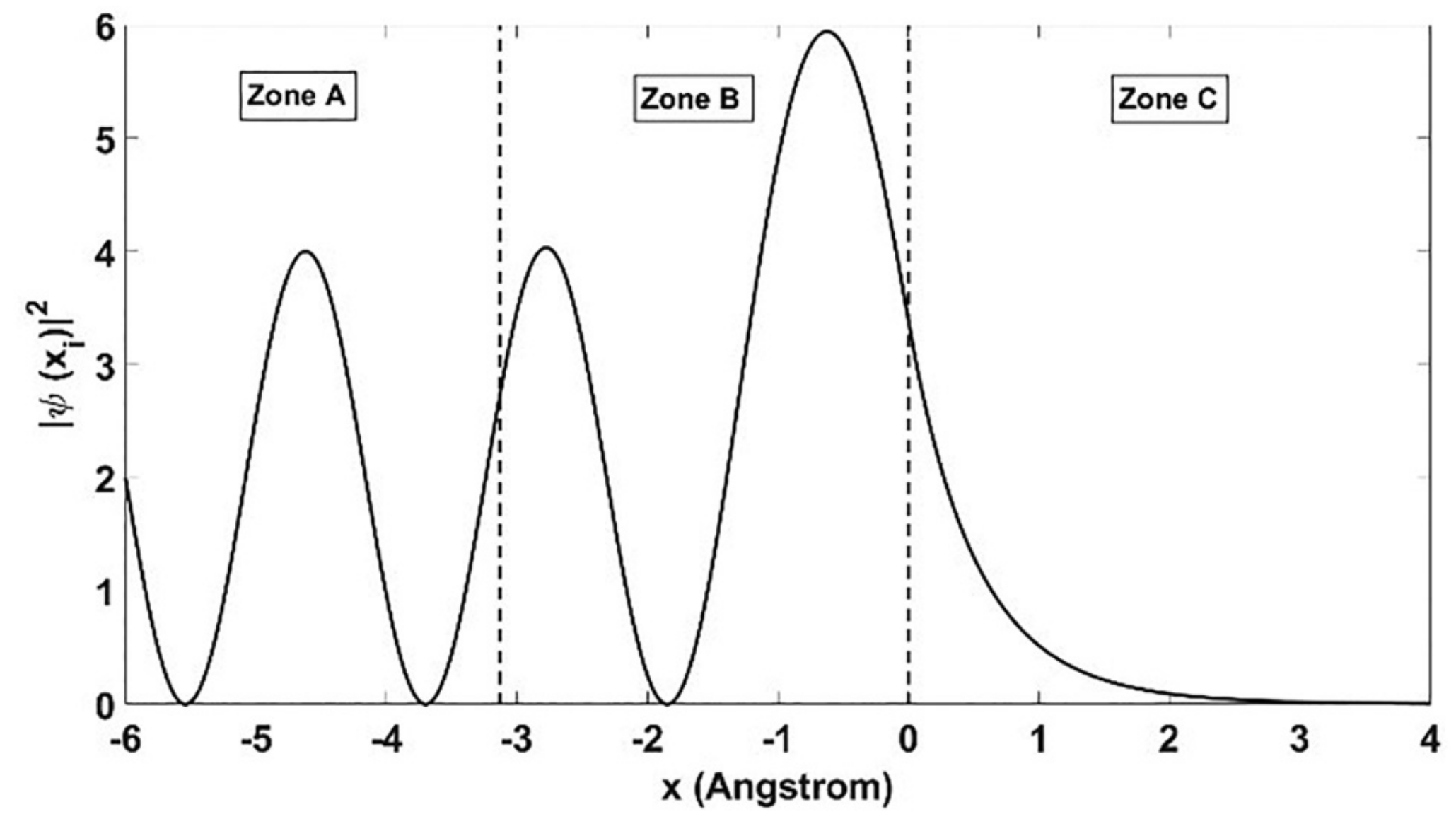

Figure 1: Plot of $|\psi(z)|^2$ as a function of position for the electronic wavefunction of (100) copper with an external field of 5 GV/m at the normal energy E_z of 7.5 eV.

Theoretical formulation

The wave functions at the metal-vacuum interface are calculated using numerical solutions of the 1D Schrodinger equation called as Numerov techique [1, 2], using this technique the transmission coefficient using boundary conditions at the interface is also calculated.

$$\psi_{i+1} = [\psi_{i-1}12 - (dz)^2 f_{i-1} - 2\psi_i 5(dz)^2 f_i + 12]/[(dz)^2 f_{i+1} - 12] \tag{1}$$

Using the electron distribution function from Monte carlo and transmission coefficient from Numerov technique, we can the find the current density as given in [1]

$$J_z = \left[\frac{q\hbar}{(2\pi^2)m}\right] \int\int k_{||} dk_{||} dk_z k_z T(k_z) f(k_{||}, k_z), \tag{2}$$

where $T(k_z)$ is the transmission coefficient and $f(k)$ is the electron distribution function.

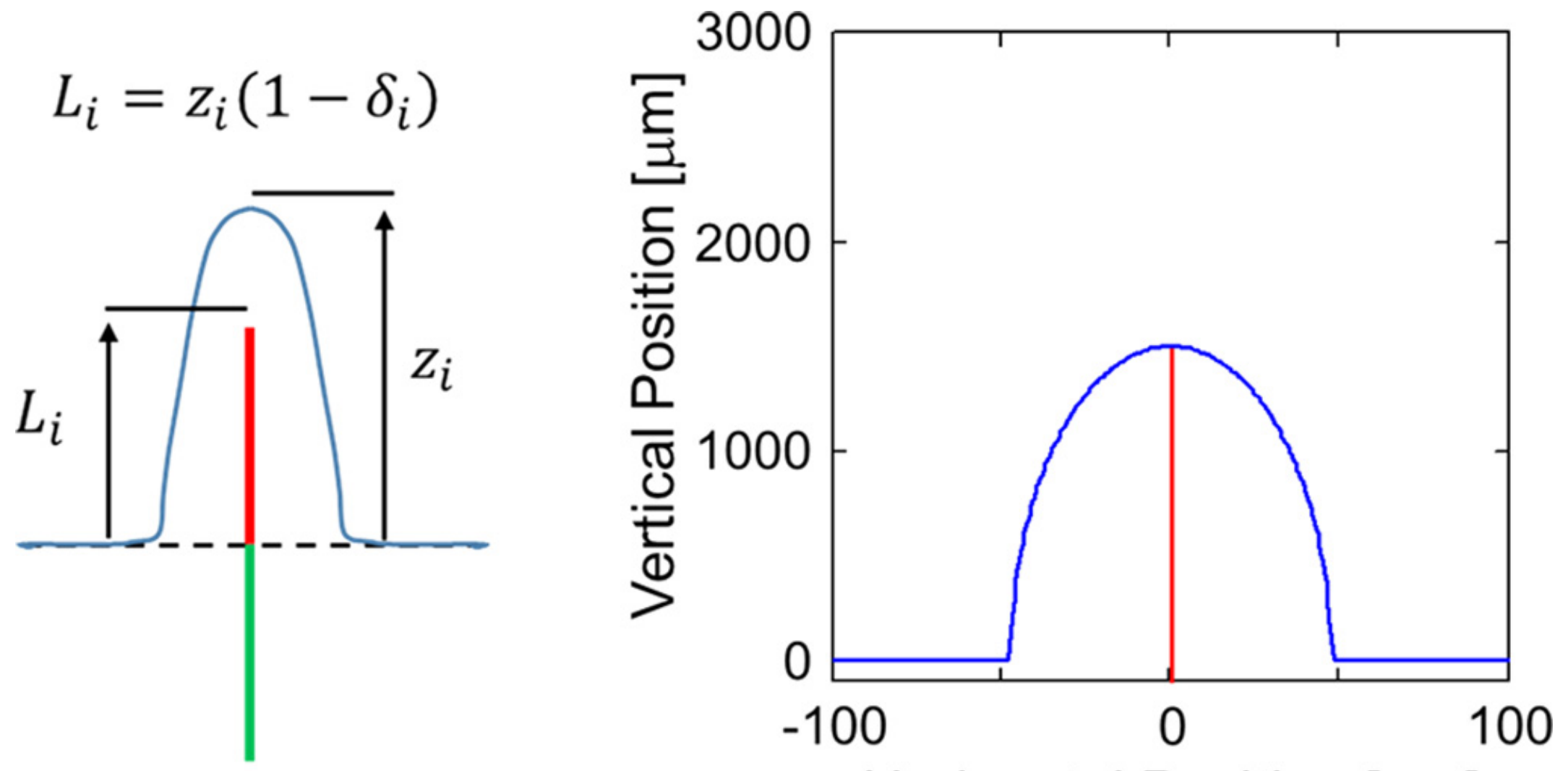

Figure 2: Line charge model (Left) Geometry, showing showing line charge(red) and image charge(green) of length L_i and resulting zero potential surface(blue) at height z_i above the goround plane. (Right) Calculated zero-potential surface for line charge with height of 1500 $\mu mandtipradiusof 1.5 \mu m$.

To further increase these current densities, we employ an array of such materials as emitters, and the potential across this array is given by [2]

$$V(\overrightarrow{r}, z) = \sum_i \frac{\lambda_i q G_i(\overrightarrow{r}, z)}{4\pi\epsilon_0} - F_0 z, \tag{3}$$

where F_0 is the applied field,

$$\lambda_i = \frac{4\pi\epsilon_0 z}{\left[z_i \ln(\frac{L_i+z_i}{-L_i+z_i}) - 2L_i\right] q}$$

and

$$G_i(\overrightarrow{r}, z) = \int_{-L}^{L} \frac{s}{\left(r^2 + (z-s)^2\right)^{\frac{1}{2}}} ds$$

.

Electron emission basics

The fundamental principles of field emission have been explored by [3].

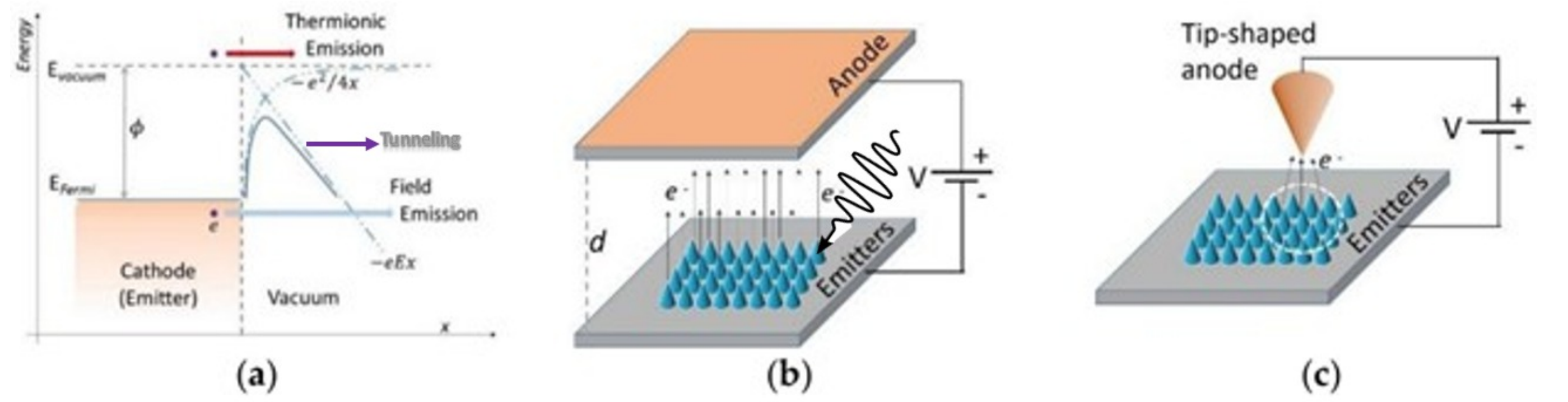

Figure 3: (a) Potential energy of electron as a function of metal-vacuum interface (b) Parallel plate and (c) Tip configuration for average and local characteration, respectively.

Simulation results

Monte carlo simulations are used to calculate electronic distribution and electron-electron and electron-phonon scattering rates, the scattering rates are based on equations given in [5].

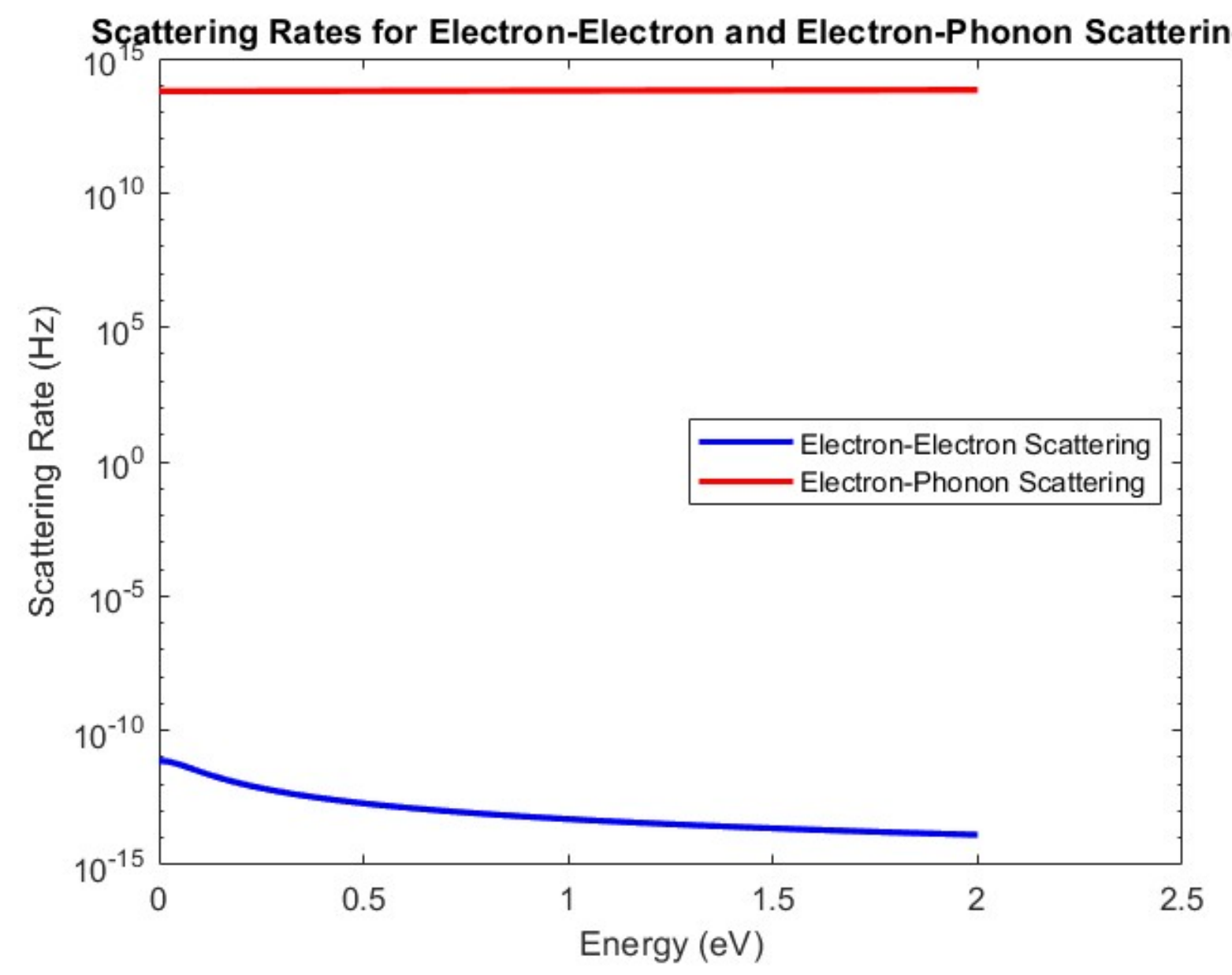

Figure 4: Electron-electron and electron-phonon scattering rates as a function of energy for copper.

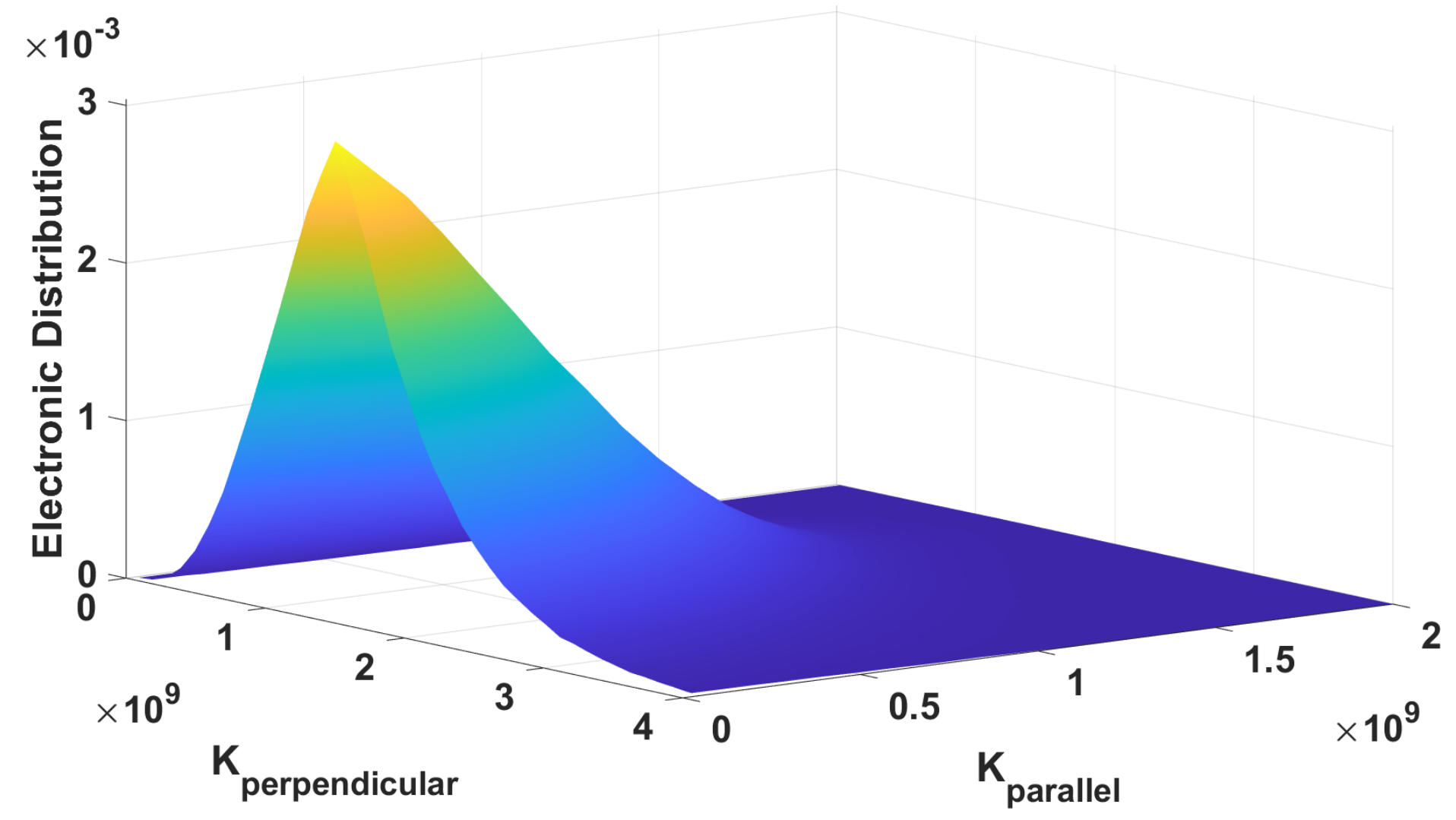

Figure 5: Electron distribution at the surface of copper as a function perpendicular and parallel momenta.

Using LCM, the current in case of a single emitter is calculated by [4].

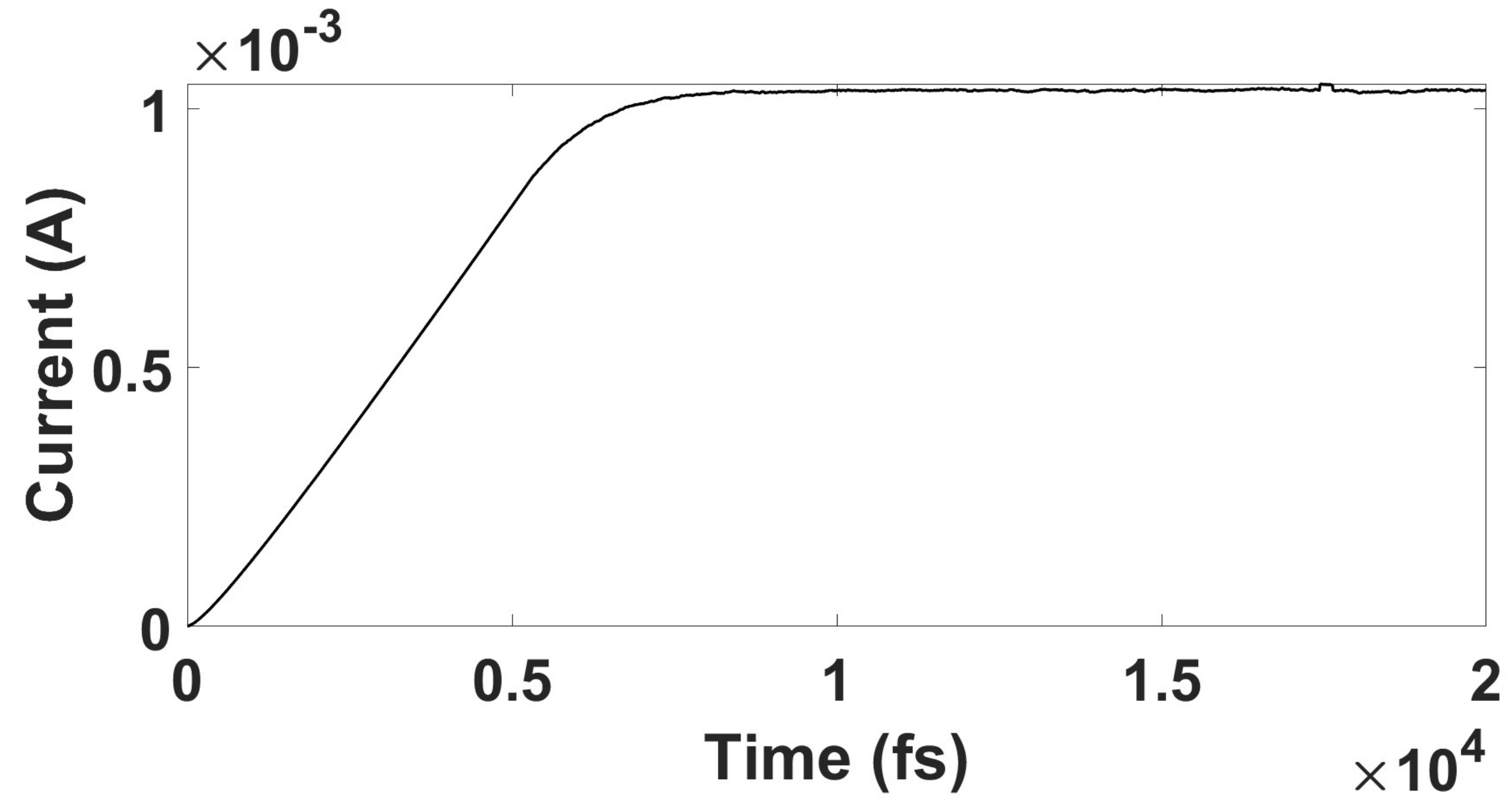

Figure 6: Time dependent total current in a single emitter with applied field 1e7 V/m and aspect ratio 1e3.

Proximity effects

The electric field strength at the emitter's tip is reduced in response to the presence of nearby emitters, and a more detailed analysis of this effect can be conducted when dealing with a smaller number of emitters [6].

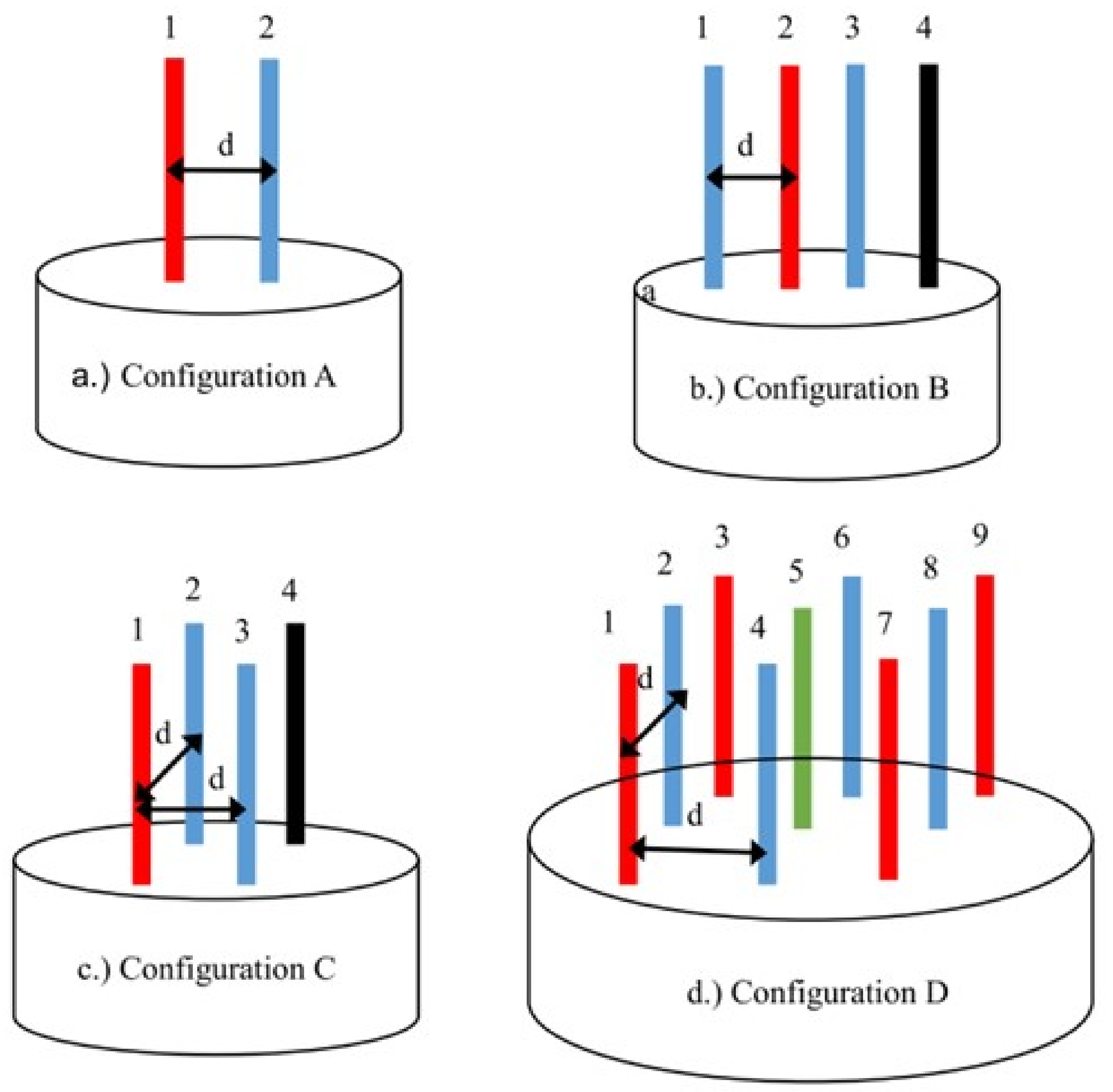

Figure 7: (a)Each fiber only sees one nearest neighbor (b) The middle fiber sees two nearest neighbors (c) Fiber 1 sees two nearest neighbors 2 and 3 and one diagonally nearest neighbor (d) Fiber 5 sees 4 nearest neighbors and 4 diagonally nearest neighbors.

Applications

This research has the potential to pave the way for the development of devices that rely on electron sources. Emitters, due to their capability to generate elevated current densities and increased pulse repetition rates, hold the promise of enabling the creation of electron beams with remarkable luminosity, substantial current density, minimal energy dispersion, all while operating at low temperatures and delivering substantial power output [1]. Some of the areas benefiting from this research include but not limited to are

- Flat panel displays
- X ray tube sources
- Cathode ray lamps
- Nanolithography
- High power microwave

References

1. S. N. Sami, L. Diaz, M. Sanati and R. P. Joshi, "Simulations of field emission from copper electrodes with inclusion of oxygen surface layer and work function changes based on first-principles calculations", *Journ. Applied Physics* **128**, 223302, (2020).
2. B. V. Numerov, "A method of extrapolation of perturbations", *Monthly Notices of the Royal Astronomical Society*, **84** (8): 592–601, (1924).
3. J. R. Harris, K. L. Jensen, D. A. Shiffler et. al, "Shielding in ungated field emitter arrays", *Appl. Phys. Lett.* **106**, 201603 (2015) .
4. F. Giubileo et. al, "Field emission from Carbon Nanostructures", *Applied Sciences*, **8**(4) , 526 (2018).
5. D. Guo, R. P. Joshi, "Simulations for Electron Emission and Maximum Current Output from Metal Emitter Arrays" , : *Journ. Applied Physics* **129**, 173301 (2021).
6. K. L. Jensen, E. J. Montgomery, D. W. Feldman, P. G. O'Shea, J. R. Harris, J. W. Lewellen, N. Moody,"Multiple scattering effects on quantum efficiency and response time for cesiated metal photocathodes", *Journal of Applied Physics* **110**, 034504 (2011).
7. W. W. Tang et. al, "Field emission characteristics of a small number of carbon field emitters", *AIP Advances* **6**, 095007 (2016).